JULY 20 2022

The chimney tube in musical acoustics: A textbook-level formulation for students and musicians[a)]

Special Collection: Education in Acoustics

Katherine L. Saenger

J. Acoust. Soc. Am. 152, 540–546 (2022)
https://doi.org/10.1121/10.0012878

JASA ARTICLE

The chimney tube in musical acoustics: A textbook-level formulation for students and musicians[a)]

Katherine L. Saenger[b)]
115 Underhill Road, Ossining, New York 10562, USA

ABSTRACT:
The chimney tube, comprising connected body and chimney segments with respective diameters d_1 and d_2, is ubiquitous in musical acoustics and can be a useful analog for flute embouchure holes, woodwind toneholes, and organ pipes. Most treatments are complex and not readily accessible to lay audiences. Simple expressions for the input impedance of ideal chimney tubes are derived by two methods. Chimneys short compared to the overall length of the resonator are shown to have effective lengths larger than their physical length by the factor $(d_1/d_2)^2$ when the chimney is open and smaller by the same factor when closed. Examples presented range from a simple cylindrical tube open at both ends to the classic Helmholtz resonator. Insights are provided about tonehole placement and the tradeoffs between a tonehole's position and diameter; how the resonance frequencies of an open-open chimney tube with a short chimney do not depend on which end is used as the input; and the interesting way in which a long chimney can change the spacing of the resonances from the 1:2:3 pattern of a cylinder open at both ends to the characteristic 1:3:5 pattern of a cylinder open at one end and closed at the other.
 https://doi.org/10.1121/10.0012878
(Received 23 January 2022; revised 17 June 2022; accepted 5 July 2022; published online 20 July 2022)
[Editor: Preston Scot Wilson] Pages: 540–546

I. INTRODUCTION

Chimney tubes, comprising connected body and chimney segments with respective diameters d_1 and d_2, are ubiquitous in musical acoustics and can provide useful analogs in settings as diverse as the embouchure hole of the flute, woodwind toneholes, and organ pipes. There is much in the literature on the input impedance of resonators with a chimney tube geometry.[1–7] However, these treatments are generally quite complex and not readily accessible to lay audiences interested in understanding, for example, why the effective length of the flute embouchure hole is longer than its physical length or how an instrument's effective length is affected by the diameter of its first open tonehole. With one possible exception,[8] even the standard musical acoustics textbooks[9–11] are a stretch for the novice reader, in part due to the choice of a 3-way junction or branched resonator as the starting point for the model structure.

This article seeks to remedy this situation by presenting a textbook-level solution and derivation for the chimney tube problem. It is hoped that the results of this exercise will be of use to both curious wind-instrument players trying to better understand the acoustics of their instruments and scientist writers in need of a semi-technical reference to cite when writing for non-specialists.

We begin with expressions for the input impedance of idealized, open-input chimney tubes shown in Figs. 1 and 2. This is followed by a look at the simplifications that result in certain special cases (e.g., chimney tubes with short chimney sections) and some of the peculiarities in the impedance spectra that one can see with certain geometries of organ chimney pipes. The ways in which real chimney tubes differ from the idealized ones of the model will be assessed and inaccuracies related to the omission of the end correction terms will be remedied. Finally, we will outline two methods of deriving the input impedance expressions on which this paper is based, leaving the details as homework problems suitable for an undergraduate musical acoustics course.

II. RESULTS AND DISCUSSION: IMPEDANCE EXPRESSIONS

The frequencies of a resonator's resonances (with f_n denoting the frequency of the nth resonance) can be found from a function known as the input impedance, designated by the expression Z_{in}/Z_c, where Z_c is the characteristic impedance, the input impedance of an infinitely long tube having a cross-sectional area S identical to that of the resonator's input aperture (which gives Z_c a value that is inversely proportional to S). A plot of the absolute value (or magnitude) of Z_{in}/Z_c (designated $|Z_{in}/Z_c|$) vs frequency is known as the input impedance spectrum; for open-input resonators, the frequencies of the resonances coincide with the minima in $|Z_{in}/Z_c|$. As will be shown in the derivations of Sec. IV, the value of Z_{in}/Z_c for the open chimney case of Fig. 1 and the closed chimney case of Fig. 2 are as follows:

[a)]This paper is part of a special issue on Education in Acoustics.
[b)]Electronic mail: klsaenger@yahoo.com

https://doi.org/10.1121/10.0012878

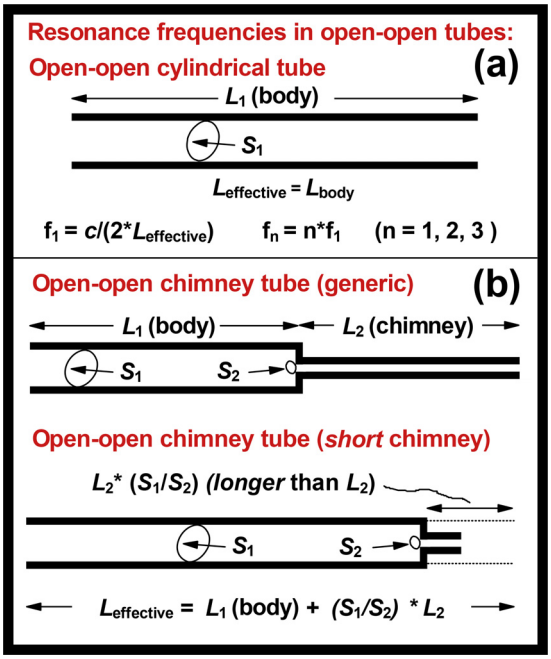

FIG. 1. (Color online) Components of the effective resonator length for open-open chimney tubes with a fundamental resonance f_1 at $c/(2L_{effective})$. Note that the effective length of the chimney is *longer* than its physical length.

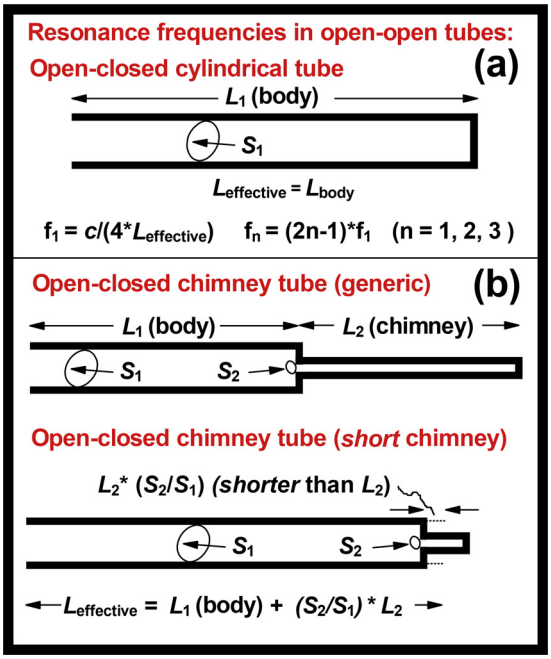

FIG. 2. (Color online) Components of the effective resonator length for open-closed chimney tubes with a fundamental resonance f_1 at $c/(4L_{effective})$. Note that the effective length of the chimney is *shorter* than its physical length.

$$\frac{Z_{in}}{Z_c}(\text{open chimney}) = i\left[\frac{\sin(kL_1)\cos(kL_2) + (S_1/S_2)\cos(kL_1)\sin(kL_2)}{\cos(kL_1)\cos(kL_2) - (S_1/S_2)\sin(kL_1)\sin(kL_2)}\right] \tag{1}$$

and

$$\frac{Z_{in}}{Z_c}(\text{closed chimney}) = -i\left[\frac{\cos(kL_1)\cos(kL_2) - (S_2/S_1)\sin(kL_1)\sin(kL_2)}{\sin(kL_1)\cos(kL_2) + (S_2/S_1)\cos(kL_1)\sin(kL_2)}\right], \tag{2}$$

where $k = 2\pi f/c$; f and c are, respectively, the frequency in Hz and the speed of sound ($\sim 3.4 \times 10^4$ cm/s); $i = \sqrt{(-1)}$; sin and cos are the trigonometric functions sine and cosine; L_1 and L_2 are the lengths of the main tube and chimney extension, respectively; and S_1 and S_2 are the cross-sectional areas of tube sections 1 and 2 (equal to $\pi d_1^2/4$ or $\pi d_2^2/4$, where d_1 and d_2 are the corresponding tube section diameters).

We look at three special cases, all directly derivable from Eqs. (1) and (2), with all but the first requiring some trigonometric identities and algebra.[12]

When there is no chimney (L_2=0),

$$\frac{Z_{in}}{Z_c}(\text{open chimney}) = i\tan(kL_1), \tag{3}$$

$$\frac{Z_{in}}{Z_c}(\text{closed chimney}) = -i\cot(kL_1). \tag{4}$$

When the chimney diameter matches the diameter of the body tube (i.e., S_2=S_1),

$$\frac{Z_{in}}{Z_c}(\text{open chimney}) = i\tan(k(L_1 + L_2)), \tag{5}$$

$$\frac{Z_{in}}{Z_c}(\text{closed chimney}) = -i\cot(k(L_1 + L_2)). \tag{6}$$

When the chimney is short enough that $kL_2 \ll 1$ (a condition reliably satisfied for the fundamental f_1 whenever $L_2 \ll L_1$), $\cos(kL_2)$ and $\cot(kL_2)$ are approximately unity and $\sin(kL_2)$ and $\tan(kL_2)$ can be replaced by kL_2,

$$\frac{Z_{in}}{Z_c}(\text{open chimney}) = i\tan(k(L_1 + (S_1/S_2)L_2)), \tag{7}$$

$$\frac{Z_{in}}{Z_c}(\text{closed chimney}) = -i\cot(k(L_1 + (S_2/S_1)L_2)). \tag{8}$$

While it is not so easy to see where the minima are in $|Z_{in}/Z_0|$ for the general case, it is quite easy for the special cases of Eqs. (3)–(8):

- The minima of $|\tan(kL)|$ occur when $kL = n\,\pi$ (with n = 1, 2, 3,…), i.e., at $f_n = n\,c/(2L)$.
- The minima of $|\cot(kL)|$ occur when $kL = (2n-1)\,\pi$ (with n = 1, 2, 3,…), i.e., at $f_n = (2n-1)\,c/(4L)$.

Because wall losses and radiation have been omitted from the calculation, the values of $|Z_{in}/Z_c|$ at these minima are equal to zero.

Equations (3) and (4) for the first special case (chimney length = 0) can be found in most acoustics textbooks

[see, for example, Ref. 10, Eqs. (8.24) and (8.25)]. Equations (7) and (8) for the special case of a short chimney, the source of the expressions in Figs. 1 and 2, are in agreement with alternative formulations of the same problem given in Ref. 11 (pp. 301–304) for a closed chimney and in Refs. 8 [Eq. (32.13)] and 11 (pp. 317–320) for an open one.

As shown schematically in Figs. 1 and 2 for chimney tubes with short chimneys, the frequency of the lowest (fundamental) resonance (f_1) depends on the effective length of the resonator, $L_{effective}$, equal to the sum of the body tube's length (L_1) and the *effective* length of the chimney. The effective length of the chimney is longer than the chimney's physical length L_2 when the chimney is open (by the factor S_1/S_2, the ratio of the body tube and chimney hole cross-sectional areas S_1 and S_2), but shorter than its physical length (by the same S_1/S_2 factor) when the chimney is closed. Consequently, $L_{effective}$ is longer than the sum of L_1 (the body length) and L_2 (the chimney length) for the chimney-open tube and shorter than this sum for the chimney-closed tube.

Equation (7) provides a useful way to better understand two aspects of woodwind instrument design: (i) the effective length of the flute embouchure hole (the part of the flute the player blows into, located in the flute's headjoint, as indicated in Fig. 3) and (ii) the way in which the sounded pitch is affected by the dimensions of the instrument's first open tonehole. This is true despite the fact that the chimney segments in these two cases are perpendicular to the main tube axis rather than perpendicular to it, as was the case for the generic chimney tubes of Figs. 1 and 2. The approximate equivalence of the perpendicular and parallel geometries is illustrated in Figs. 3(b) and 3(c) for the case of the embouchure hole in the flute headjoint.

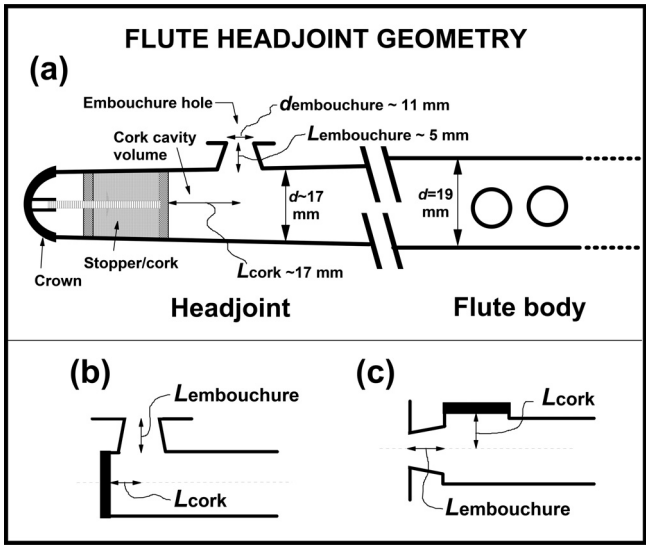

FIG. 3. Cross-section schematics of flute headjoint geometry: (a) headjoint components (including a portion of the flute body to which the headjoint is attached) and critical dimensions; (b) a close-up view of an idealized headjoint with a much-reduced cork cavity volume; (c) the headjoint of (b) with the cork cavity and embouchure hole reversed to emphasize the resemblance of the flute headjoint to a chimney tube.

The effective length of the flute's embouchure hole is longer than its physical length. As a result, the effective length of the instrument is significantly longer than the distance between the embouchure hole and the first open tonehole. How does this come about? Looking at Fig. 3(a), one sees that the flute headjoint has a diameter of ~17 mm at the position of the embouchure hole (reduced from the 19 mm diameter of the flute body due to the headjoint taper). The embouchure hole has a depth L_2 of ~5 mm and a cross-sectional area S_2 that is about 30%–40% of the cross-sectional area of the flute body S_1 (based on an embouchure hole that has the shape of a rounded rectangle, ~10 mm across by ~12 mm wide). This gives a S_1/S_2 ratio of ~3 for the bare embouchure hole. However, the player's lips cover about 40% of the embouchure hole area (reducing S_2 to about 60% of its nominal value) and act as a one-sided extension of the embouchure hole wall (increasing the value of L_2 from a value of 0.5 cm to perhaps 1.0 cm). This leads to an effective embouchure hole length of 1.0 cm × (3/0.6) = 5 cm, in reasonable agreement with the values of ~5 cm suggested in Ref. 9 (p. 495) for low frequencies (with no consideration of the cork cavity) and the frequency-dependent 3 to 5 cm suggested by Ref. 10 (p. 541) for the quasi-zero-volume cork cavity case in which the cork stopper is pushed into the point where it begins to obstruct the embouchure hole.[13]

Regarding woodwind toneholes, the effect of tonehole placement is clear even without Eq. (7): moving the tonehole away from the instrument's input aperture increases the instrument's effective length, and lowers the pitch of the played note. However, Eq. (7) points to how an instrument's sounded pitch is affected by tonehole dimensions. Just as with the case of the flute embouchure hole, each tonehole has an effective length that contributes to the instrument's total effective length when that tonehole is the first one open. Increasing the diameter of the first open tonehole decreases its effective length; to keep the same intonation, the center of the modified tonehole must therefore be moved further away from the embouchure hole. In instruments such as baroque flutes and recorders with relatively small toneholes in a thick-walled body, the tonehole's effective length can be quite significant.

III. RESULTS AND DISCUSSION: IMPEDANCE PLOTS

Here we take a look at the predictions of Eqs. (1)–(8) for various cases of interest and compare them to a "full-strength" matrix method computation which fully includes the complicating factors of the frequency-dependent end corrections, losses from radiation, and losses from molecular interactions with the resonator's walls.[14] Because the resonances for open-input tubes occur at input impedance minima, we plot the inverse of the input impedance, known as the input admittance $|Z_c/Z_{in}|$, so that the resonances show up as peaks.

Figure 4 shows $|Z_c/Z_{in}|$ for the case of a plain (no chimney) cylindrical tube that is either open at its far end

https://doi.org/10.1121/10.0012878

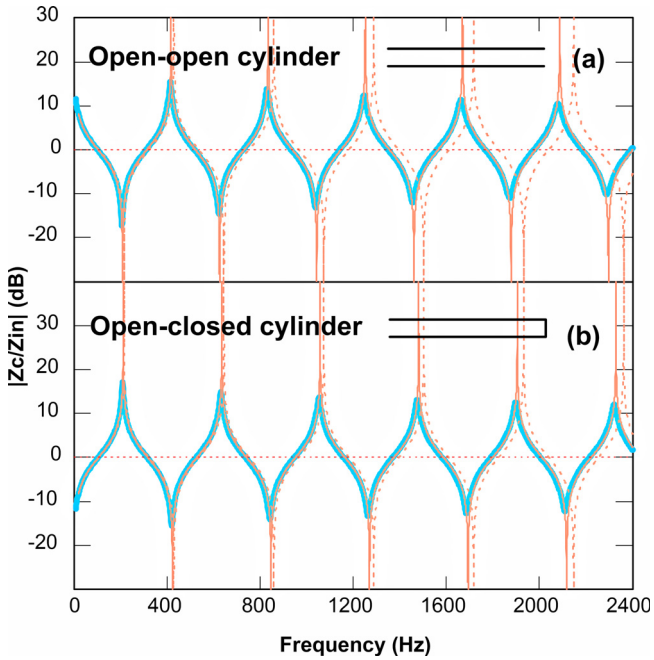

FIG. 4. (Color online) Spectra for (a) an open-open cylindrical tube and (b) an open-closed cylindrical tube of length $L_1 = 40$ cm and diameter d_1=1.9 cm. Wide lines, full-strength computation of Ref. 14 with wall losses (1.0× theoretical), radiation losses, and end corrections. Thin lines, predictions of Eqs. (3) and (4), with (solid) and without (dotted) end corrections. The dB scale is amplitude based (i.e., 10 log$|Z_c/Z_{in}|$).

[Fig. 4(a)] or closed at its far end [Fig. 4(b)]. The wide traces show the full-strength simulation and the thin dotted traces show the predictions of Eqs. (3) and (4). Both sets of spectra show approximately equally spaced maxima (peaks) with minima (valleys), with peaks at the expected f_1, $2f_1$, $3f_1$, etc., positions for the open-open tube and f_1, $3f_1$, $5f_1$, etc., positions for the open-closed tube. Note also that the spectral contrast (vertical spacing between minima and maxima) is very much reduced in the full-strength calculations due to the inclusion of the wall loss and radiation loss terms; the fact that these losses increase with frequency is responsible for the gradual falloff in spectral contrast seen as one moves from the lowest resonance to the highest.

However, the dotted thin line traces from expressions of Eqs. (3) and (4) consistently overestimate the frequencies of the minima and maxima. This is due to the omission of the usual end correction, a length term that needs to be added to each open end of the resonator. The end correction is frequency dependent and has a value that is around 0.3× the tube diameter. The thin line traces include a more accurate expression [Eq. (14a) of Ref. 15] for these end corrections and bring the frequencies of the extrema into good agreement with those of the full-strength calculation.

The tubes of Figs. 4(a) and 4(b) also show the expected factor of 2 difference in their f_1 values, a consequence of f_1 being $c/(2L)$ for the open pipe and $c/(4L)$ for the closed one. Incidentally, a pedagogically interesting example of a transition from an open pipe to a closed one can be performed with a flute headjoint. The experimenter first listens to the pitch produced by blowing the headjoint by itself (no flute body). The player then sticks a finger into the end of the headjoint to shorten the air column length. Paradoxically, this lowers the pitch rather than raises it, due to the fact that the end of the tube is no longer open when the finger is fully inserted.

The tubes of Figs. 4(a) and 4(b) also show the expected factor of 2 difference in their f_1 values, a consequence of f_1 being $c/(2L)$ for the open pipe and $c/(4L)$ for the closed one. Incidentally, a pedagogically interesting example of a transition from an open pipe to a closed one can be performed with a flute headjoint. The experimenter first listens to the pitch produced by blowing the headjoint by itself (no flute body). The player then sticks a finger into the end of the headjoint to shorten the air column length. Paradoxically, this lowers the pitch rather than raises it, due to the fact that the end of the tube is no longer open when the finger is fully inserted.

Figure 5 shows $|Z_c/Z_{in}|$ for the case of an open-open tube with a short chimney, where the wide traces are again for the full-strength calculations and the thin lines are for the Eq. (1) expression with the end corrections included. The upper section is for a chimney tube with the orientation of the tube in Fig. 1(a); the lower section is for the same exact tube but with the input and output switched (i.e., the input is now at the end of the short, narrow chimney). Interestingly, the frequencies of the peaks are identical for both chimney tube orientations, while the shape of the peaks and the positions of the minima are quite different. The thin dotted line is for the short chimney approximation of Eq. (7), i.e., for the case of a simple cylindrical tube of

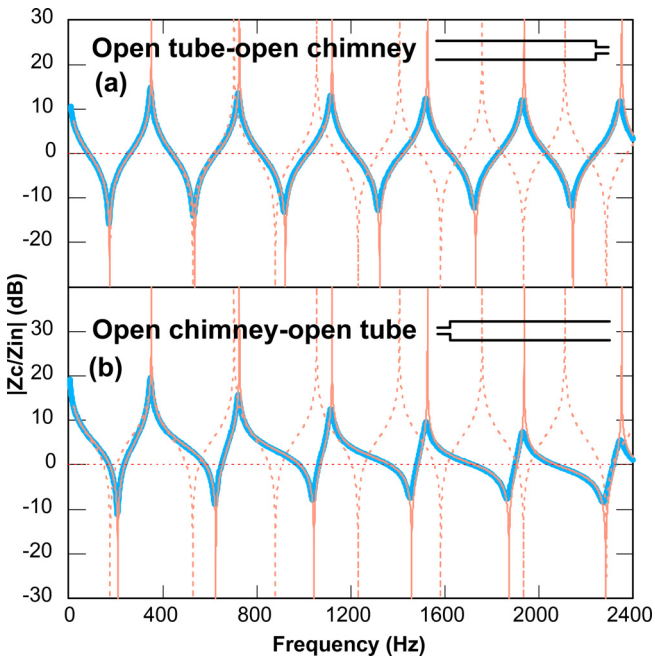

FIG. 5. (Color online) Spectra for an open-open chimney tube with a main section length/diameter $L_1/d_1 = 40/1.9$ cm and a chimney L_2/d_2 of 2.0/0.95 cm (a); the same tube with the input and output switched (b). Wide lines, full-strength computation of Ref. 14 with wall losses (1.0× theoretical), radiation losses, and end corrections. Thin lines, the predictions of Eq. (1), with end corrections (solid); the predictions of Eq. (7) with end corrections (dotted). The dB scale is amplitude based (i.e., 10 log$|Z_c/Z_{in}|$).

diameter d_1 and length $L_1 + (S_1/S_2)L_2$, using end corrections based on the original d_1 and d_2 values. As expected, this approximation shows regularly spaced peaks at 1, 2, 3, etc., at multiples of a common fundamental. However, the upper resonances for the real chimney tube show a systematic displacement to frequencies higher than nf_1.

In a final example, Fig. 6 shows $|Z_c/Z_{in}|$ for two cases of chimney tubes not amenable to simplifying approximations. As before, the wide traces are for the full-strength calculations and the thin lines are for the applicable Eq. (1) or (2) expressions with the end corrections included. The first case [Fig. 6(a)] is for an organ pipe similar to ones studied in Ref. 7, with an overall length of ~80 cm, body to chimney length ratio L_1/L_2 of ~3, and diameter ratio d_1/d_2 of ~4. The long narrow chimney tends to shift the resonances from the classic 1:2:3 ratio for an open-open cylindrical tube toward the classic 1:3:5 ratio of an open-closed cylinder. The positions of the resonances have no simple pattern; organ makers and pipe designers attempt to optimize the placement of the resonances so that the f_3 or f_5 line up with $3f_1$ or $5f_1$.[7]

The second case [Fig. 6(b)] is for a reversed open-closed chimney pipe studied in Ref. 14, comprising a chlorinated polyvinyl chloride (CPVC) chimney and a polyvinyl chloride (PVC) body tube. The open chimney (now with dimensions L_1 and d_1) is at the input, and the body tube to which it is connected (now with dimensions L_2 and d_2) is closed at its far end. This chimney pipe had an overall length of ~32 cm, body-to-chimney length ratio of ~2, and body-to-chimney diameter ratio of ~2.2; it is included in this paper because the same full-strength model shown in the plots (though with a wall loss term multiplied by 1.3 to account for wall roughness) provided an excellent fit to the experimentally measured resonance spectrum.

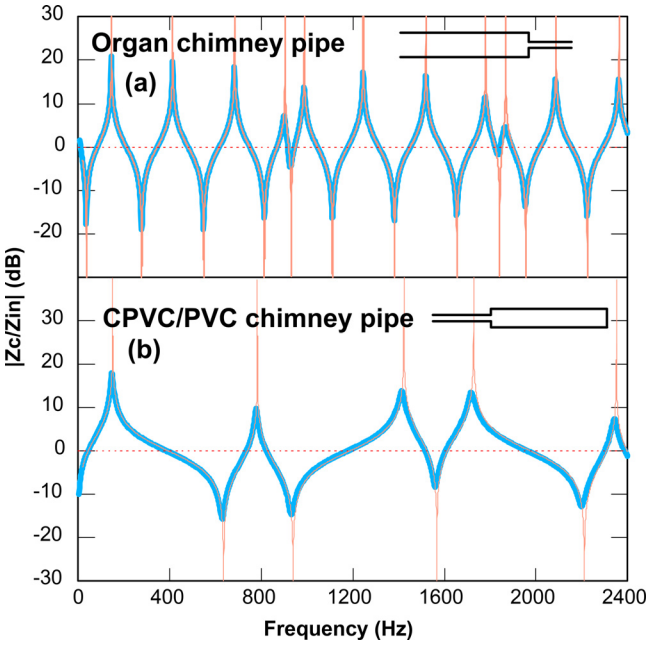

FIG. 6. (Color online) Spectra for two chimney pipes: a generic open-open organ chimney pipe with body L_1/d_1 of 60/7.9 cm and chimney L_2/d_2 of 18/1.9 cm (a); and an experimental open-closed CPVC/PVC chimney pipe with a chimney L_1/d_1 of 10.45/1.2 cm and a body L_2/d_2 of 21.95/2.58 cm (b). Wide lines, full-strength computation of Ref. 14 with wall losses, radiation losses, and end corrections, where wall losses are 1.0× theoretical for (a) and 1.3× theoretical for (b). Thin lines, predictions of Eqs. (1) or (2), with end corrections. The dB scale is amplitude based (i.e., $10\log|Z_c/Z_{in}|$).

It is interesting to note that the chimney tube resonator of Fig. 6(b) is quite similar in shape to the much-studied[6] structure known as a Helmholtz resonator. Helmholtz resonators have an open-closed geometry and comprise a closed, hollow body section of volume V connected to a short and narrow open neck section. With a sufficient shortening of the Fig. 6(b) resonator's narrow chimney section, the correspondence between the two resonator structures is arguably exact. The textbook expression (see, for example, Ref. 10, p. 14) for the fundamental frequency of a Helmholtz resonator with neck dimensions L_1 and S_1 and body volume $V_2 = L_2S_2$ is $f_1 = (c/2\pi)\sqrt{(S_1/(L_1V_2))}$. It is therefore satisfying to know that the identical result can be directly derived from the Eq. (2) expression for an open–closed chimney tube: set Eq. (2) to zero and solve for k with the cos terms approximated as unity and the sin terms approximated as kL_1 or kL_2.

IV. BASIC DERIVATION OF CHIMNEY TUBE IMPEDANCE

Here we derive Eq. (1) starting from Eq. (8.23) of Ref. 10 for the input impedance for an idealized cylindrical pipe 1 of length L_1 and cross-sectional area S_1:

$$Z_{in_1} = Z_{c_1}\left[\frac{Z_{out_1}\cos(kL_1) + iZ_{c_1}\sin(kL_1)}{iZ_{out_1}\sin(kL_1) + Z_{c_1}\cos(kL_1)}\right], \tag{9}$$

where Z_{out_1} is the impedance at the output end of the pipe and $Z_{c_1} = \rho c/S_1$ is the characteristic impedance of pipe 1, where ρ is the density of air and c is the speed of sound. When the end of pipe 1 is closed, $Z_{out_1} = \infty$, and Eq. (9) reduces to

$$Z_{in_1}(\text{closed pipe 1}) = -iZ_{c_1}\cot(kL_1). \tag{10}$$

When the end of pipe 1 is ideally open, $Z_{out_1} = 0$, and Eq. (9) reduces to

$$Z_{in_1}(\text{open pipe 1}) = iZ_{c_1}\tan(kL_1). \tag{11}$$

If there is a chimney (i.e., a second pipe) of length L_2 and cross-sectional area S_2 at the output of the first pipe, the quantity Z_{out_1} is simply given by the right side of Eq. (10) or (11), depending on whether the chimney is closed or open, with Z_{c_2} (equal to $\rho c/S_2 = (S_1/S_2)\cdot Z_{c_1}$) and L_2 substituted for Z_{c_1} and L_1, e.g.,

$$\begin{aligned} Z_{out_1}(\text{open pipe 2}) &= iZ_{c_2}\tan(kL_2) \\ &= i(S_1/S_2)\cdot Z_{c_1}\tan(kL_2). \end{aligned} \tag{12}$$

Equation (13) shows Eq. (9) with the substitutions for a chimney that is open,

https://doi.org/10.1121/10.0012878

$$\frac{Z_{\text{in}}}{Z_{c_1}}(\text{open chimney pipe}) = \left[\frac{i\left(\frac{S_1}{S_2}\right)\cdot Z_{c_1}\tan(kL_2)\cos(kL_1) + iZ_{c_1}\sin(kL_1)}{-\left(\frac{S_1}{S_2}\right)\cdot Z_{c_1}\tan(kL_2)\sin(kL_1) + Z_{c_1}\cos(kL_1)}\right]. \tag{13}$$

Equation (1) can then be obtained from Eq. (13) with a minor rearrangement.

V. MATRIX DERIVATION OF CHIMNEY TUBE IMPEDANCE

The pressure-based transfer matrix method (TMM) of Ref. 14 is more general and is particularly useful for quasi-one-dimensional tubular resonators (such as the modern flute) having geometries that are more complex, but still describable in terms of cylindrical tube segments in combination with open and closed branches. It is very tedious to get from the starting TMM equations to Eqs. (1) and (2), but the process is straightforward.

The quantities being evaluated are the amplitudes of the forward-going and backward-going pressure waves, P_{n}^{+} and P_{n}^{-}, in each tube segment n. Using the two-segment chimney tube geometries shown in Figs. 1 and 2, the quantities of interest are P_{n}^{+} and P_{n}^{-} with $\text{n}=1$, 2, and 3 corresponding, respectively, to tube segment 1, tube segment 2, and the ambient at the output end of the tube. When the chimney portion of the chimney tube is open, P_3^{+} is not initially known and P_3^{-} is zero (since there is no back-reflected wave in the outside ambient); when the chimney is closed, P_3^{+} is zero (since nothing is going into the outside ambient) and P_3^{-} is initially unknown.

The input impedance for the resonator is given by

$$\frac{Z_{\text{in}}}{Z_{\text{c}}} = \frac{1+\frac{P_1^{-}}{P_1^{+}}}{1-\frac{P_1^{-}}{P_1^{+}}}. \tag{14}$$

The quantities P_1^{+} and P_1^{-} are found from the deceptively simple equation

$$\begin{pmatrix} P_1^{+} \\ P_1^{-} \end{pmatrix} = \frac{C_2\,C_3}{t_2\,t_3}\begin{pmatrix} P_3^{+} \\ P_3^{-} \end{pmatrix}, \tag{15}$$

where

$$C_2 = \begin{pmatrix} e^{ikL_1} & r_2 e^{ikL_1} \\ r_2 e^{-ikL_1} & e^{-ikL_1} \end{pmatrix}, \tag{16}$$

$$C_3 = \begin{pmatrix} e^{ikL_2} & r_3 e^{ikL_2} \\ r_3 e^{-ikL_2} & e^{-ikL_2} \end{pmatrix}, \tag{17}$$

$$r_{\text{j}} = \frac{P_{\text{j}-1}^{-}}{P_{\text{j}-1}^{+}} = \frac{S_{\text{j}-1}-S_{\text{j}}}{S_{\text{j}-1}+S_{\text{j}}}, \tag{18}$$

and

$$t_{\text{j}} = \frac{P_{\text{j}}^{+}}{P_{\text{j}-1}^{+}} = \frac{2S_{\text{j}-1}}{S_{\text{j}-1}+S_{\text{j}}}, \tag{19}$$

where $S_3 = 0$ for the closed chimney tube, $S_3 = \infty$ for the open chimney tube, and Eqs. (18) and (19) are evaluated for $\text{j}=2$ and $\text{j}=3$. More detail on the general version of this method, suitable for an arbitrarily large number of tube segments and fully accounting for radiation and wall losses, can be found in the original reference.[14]

VI. CONCLUDING REMARKS

The present analysis has limitations: it omits radiation and wall losses, neglects the effects of the discontinuity of the bore where the chimney and main tube sections meet (an issue which can be treated, when necessary, by introducing inner end corrections[3] and/or modal expansion/decomposition[5,11]), and ignores the fact that the 1-dimensional models are not always well suited to geometries in which the tube segment lengths are not substantially longer than their diameters. It is hoped that the present treatment of the chimney tube will be found useful both as a guide to the intuition and as a stepping stone to the more complex treatments in the literature [as well as to a treatment buried in Ref. 11 (pp. 317–320) that is arguably equivalent to the present one].

[1]F. C. Karal, "The analogous acoustical impedance for discontinuities and constrictions of circular cross section," J. Acoust. Soc. Am. **25**, 327–334 (1953).
[2]U. Ingard, "On the theory and design of acoustic resonators," J. Acoust. Soc. Am. **25**, 1037–1061 (1953).
[3]C. J. Nederveen, J. K. M. Jansen, and R. R. van Hassel, "Corrections for woodwind tone-hole calculations," Acta Acust. Acust. **84**, 957–966 (1998), available at https://www.ingentaconnect.com/content/dav/aaua/1998/00000084/00000005/art00021.
[4]S. Kokkelmans, M.-P. Verge, A. Hirschberg, A. P. J. Wijnands, and R. L. M. Schoffelen, "Acoustic behavior of chimney pipes," J. Acoust. Soc. Am. **105**, 546–551 (1999).
[5]V. Dubos, J. Kergomard, A. Khettabi, J.-P. Dalmont, D. H. Keefe, and C. J. Nederveen, "Theory of sound propagation in a duct with a branched tube using modal decomposition," Acta. Acust. Acust. **85**, 153–169 (1999), available at https://www.ingentaconnect.com/content/dav/aaua/1999/00000085/00000002/art00003.
[6]R. L. Panton and J. M. Miller, "Resonant frequencies of cylindrical Helmholtz resonators," J. Acoust. Soc. Am. **57**, 1533–1535 (1975).
[7]P. Rucz, T. Trommer, J. Angster, A. Miklós, and F. Augusztinovicz, "Sound design of chimney pipes by optimization of their resonators," J. Acoust. Soc. Am. **133**, 529–537 (2013).
[8]C. J. Nederveen, *Acoustical Aspects of Woodwind Instruments* (Northern Illinois University Press, DeKalb, IL, 1998).
[9]A. H. Benade, *Fundamentals of Musical Acoustics* (Oxford University Press, New York, 1976).
[10]N. H. Fletcher and T. D. Rossing, *The Physics of Musical Instruments*, 2nd ed. (Springer, New York, 1999).
[11]A. Chaigne and J. Kergomard, *Acoustics of Musical Instruments* (Acoustical Society of America, New York, 2016).

[12]Hint: Use the trigonometric identity $\tan(\alpha+\beta) = [\tan(\alpha)+\tan(\beta)]/[1-\tan(\alpha)\cdot\tan(\beta)]$ with $\alpha = kL_1$ and $\beta = kL_2$ for Eqs. (5) and (6). For Eqs. (7) and (8), use the same identity with $\alpha = kL_1$ and $\beta = k\Delta L$, where ΔL is the effective length of the chimney.
[13]A more common approach to these calculations calculates the effective length of the embouchure hole in combination with the cork cavity volume. This approach, touched on in Ref. 8 (Sec. 24) and described in Ref. 10 (pp. 539–541), treats the cork cavity, embouchure hole, and flute tube resonator as a 3-way junction. It is preferred when considering more

realistic values of the cork cavity length (typically ∼17 mm) and when accurate values are desired over a wider frequency range.

[14]K. L. Saenger, "A pressure-based transfer matrix method and measurement technique for studying resonances in flutes and other open-input resonators," J. Acoust. Soc. Am. **147**, 2556–2569 (2020).

[15]J.-P. Dalmont, C. J. Nederveen, and N. Joly, "Radiation impedance of tubes with different flanges: Numerical and experimental investigations," J. Sound Vib. **244**, 505–534 (2001). The expression given for the end correction of an unflanged tube is $0.633 \cdot a \cdot [(1 + 0.044\,(ka)^2)/(1 + 0.19\,(ka)^2)]$, where a is the tube radius.